Am J Physiol Lung Cell Mol Physiol 321: L50–L64, 2021.
First published May 5, 2021; doi:10.1152/ajplung.00042.2020

american physiological society

AMERICAN JOURNAL OF PHYSIOLOGY
LUNG CELLULAR AND MOLECULAR PHYSIOLOGY

RESEARCH ARTICLE

Inter-Organ Communication in Homeostasis and Disease

Lung metabolomics after ischemic acute kidney injury reveals increased oxidative stress, altered energy production, and ATP depletion

Sophia L. Ambruso,[1,2] Hyo-Wook Gil,[3] Benjamin Fox,[2] Bryan Park,[2] Christopher Altmann,[2] Rushita A. Bagchi,[2] Peter R. Baker II,[2] Julie A. Reisz,[2] and Sarah Faubel[1,2]

[1]*Rocky Mountain Regional VA Medical Center, Denver, Colorado;* [2]*University of Colorado Anschutz Medical Campus, Denver, Colorado; and* [3]*Soonchunhyang University Cheonan Hospital, Cheonan, ChungcheongNam-do, Republic of Korea*

Abstract

Acute kidney injury (AKI) is a complex disease associated with increased mortality that may be due to deleterious distant organ effects. AKI associated with respiratory complications, in particular, has a poor outcome. In murine models, AKI is characterized by increased circulating cytokines, lung chemokine upregulation, and neutrophilic infiltration, similar to other causes of indirect acute lung injury (ALI; e.g., sepsis). Many causes of lung inflammation are associated with a lung metabolic profile characterized by increased oxidative stress, a shift toward the use of other forms of energy production, and/or a depleted energy state. To our knowledge, there are no studies that have evaluated pulmonary energy production and metabolism after AKI. We hypothesized that based on the parallels between inflammatory acute lung injury and AKI-mediated lung injury, a similar metabolic profile would be observed. Lung metabolomics and ATP levels were assessed 4 h, 24 h, and 7 days after ischemic AKI in mice. Numerous novel findings regarding the effect of AKI on the lung were observed including *1*) increased oxidative stress, *2*) a shift toward alternate methods of energy production, and *3*) depleted levels of ATP. The findings in this report bring to light novel characteristics of AKI-mediated lung injury and provide new leads into the mechanisms by which AKI in patients predisposes to pulmonary complications.

acute kidney injury; glutathione; inflammatory lung injury; metabolomics; organ cross talk

INTRODUCTION

Acute kidney injury (AKI) is a common complication, occurring in 20% of hospitalized patients (1) and 30%–50% of admissions to the intensive care unit (ICU) (2). Although previously thought to be a benign condition, AKI is now recognized to be independently associated with increased mortality (3, 4) and associated with numerous adverse clinical outcomes (5–9). Respiratory complications are particularly common and assocaited with increased mortality (10). Respiratory complications that are associated with AKI include respiratory failure, prolonged mechanical ventilation, and prolonged venilator weaning (11–15). The role AKI plays in respiratory complications has been recognized for over 100 yr and is not sufficiently explained by traditional complications of AKI such as fluid overload (16). Autopsy studies have demonstrated that AKI is associated with lung inflammation akin to that observed during acute respiratory distress syndrome (ARDS) (17, 18). Inflammation is central to the pathogenesis of ARDS and is characterized by increased circulating proinflammatory cytokines, lung chemokine upregulation, neutrophil accumulation, and neutrophil activation (16). Similarly, animal studies in AKI have demonstrated that AKI is associated with systemic inflammation and inflammatory lung injury that is characterized by increased circulating proinflammatory cytokines, lung chemokine upregulation, lung neutrophil accumulation, and increased vascular permeability (17, 19–22).

The generation of reactive oxygen species (ROS) is a consequence of living in an oxygen rich environment and elaborate mechanisms to regulate both ROS production and elimination exist. The role of the lung is to provide a large surface area (~80–100 m^2) for gas exchange and oxygen delivery for energy production; thus, the lungs are continuously exposed to high partial pressures of oxygen, and ~2% of inhaled oxygen is oxidized to yield potentially harmful ROS (23). Antioxidant defenses to keep ROS levels in check are essential for lung health. Unchecked ROS production has numerous consequences, including but not limited to, upregulation of proinflammatory cytokines and adhesion molecules, recruitment of neutrophils and macrophages, direct and indirect endothelial and epithelial barrier dysfunction, inflammatory cell penetration and fluid extravasation, irreversible modification of proteins and nucleic

Correspondence: S. L. Ambruso (sophia.ambruso@cuanschutz.edu).
Submitted 7 February 2020 / Revised 21 April 2021 / Accepted 29 April 2021

1040-0605/21 Published by the American Physiological Society.

acids, mitochondrial dysfunction with impaired oxidative phosphorylation, mitochondrial death, and cellular injury and/or death (24). Increased ROS production and oxidative stress are a consequence of inflammatory lung injury (25–28) and central to the pathogenesis of ARDS (24). The effect of AKI on lung oxidative stress has not previously been assessed.

Normally, lung tissue is a modest consumer of energy in comparison to other working tissues in the body, e.g., cardiac or skeletal tissue, but like other metabolically active tissues, eighty percent of lung ATP generation is due to mitochondrial respiration (oxidative phosphorylation) and 20% is due to other sources (29). When under stress, however, lung metabolism and energy consumption change. Murine models of inflammatory lung injury are characterized by metabolic profiles consistent with altered energy production and reduced levels of ATP (30–32). The effect of AKI on energy metabolism and ATP production in the lung has not previously been assessed.

In the present study, metabolomics assessment and ATP levels were determined in the lung at 4 and 24 h as well as 7 days after ischemic AKI in mice. To our knowledge, there are no studies that have evaluated metabolomics and energy production in the lung after AKI. We hypothesized that based on the parallels between inflammatory acute lung injury and AKI-mediated lung injury, there would be metabolomic patterns consistent with increased oxidative stress, use of alternative energy sources, and reduced energy production in the lung following AKI.

MATERIALS AND METHODS

Animals

Adult (8–10 wk old), male C57B/6 mice (Jackson Laboratories, Bar Harbor, ME), weighing between 20–25 g were used. They were maintained on a standard diet and water was freely available. All experiments were conducted in adherence to the National Institutes of Health Guide for the Care and Use of Laboratory Animals. The animal protocol was approved by the Animal Care and Use Committee of the University of Colorado, Denver.

Surgical Protocol

To induce ischemic AKI (33), mice were anesthetized with intraperitoneal avertin (2,2,2-tribromoethanol; Sigma Aldrich, Milwaukee, WI), a laparotomy was performed, and both renal pedicles were clamped for 22 min. Mice received 500 μL saline with buprenex subcutaneous injection preceding surgery and 500 μL saline was administered by subcutaneous injection daily after surgery. The sham procedure is similar in all respects—including laparotomy—except that renal pedicle clamping is not performed.

Collection and Preparation of Plasma and Lung Samples

Blood was obtained via cardiac puncture and centrifuged at 3,000 *g* at 4°C for ten minutes; plasma was collected and centrifuged a second time at 3,000 *g* for 1 min. The lungs were collected, weighed, snap frozen in liquid nitrogen, and stored at −80°C. In this experiment, lung, heart, kidney and liver were all rapidly collected and snap frozen for future metabolomics assessment (34); in order to limit time to freezing (and potential changes in metabolic phenotype due to death), no additional processing of tissue occurred and organs were not perfused before collection.

Metabolomics Analyses

Frozen lung tissue was milled with mortar and pestle in the presence of liquid nitrogen and weighed to the nearest 0.1 mg. At a tissue concentration of 10 mg/mL, the samples were extracted in ice-cold lysis/extraction buffer (5:3:2 MeOH: MeCN:water v/v/v) followed by agitation at 4°C for 30 min and centrifugation at 18,213 *g* for 10 min at 4°C. The supernatants (10 uL per injection) were immediately analyzed via ultra-high-pressure liquid chromatography coupled to online mass spectrometry (UHPLC-MS) on a Dionex UltiMate3000 and Thermo Q Exactive MS. Metabolites were resolved over a Kinetex C18 column (Phenomenex, 2.1 × 150 mm, 1.7 μm) on a 3-min isocratic method in positive and negative ion modes (separate runs) as previously described (35). Raw files were converted to .mzXML using MassMatrix and metabolites annotated and integrated using Maven (Princeton University) in conjunction with the KEGG database and an in-house standard library. Quality control was performed as previously described (36). This untargeted UHPLC-MS-based metabolomics analysis provided the measurement of 132 annotated metabolites in the lung.

Creatinine and BUN Assay

Serum creatinine was determined using the Point creatinine assay (#C7548) according to the manufacturer's directions; BUN was determined using the Bioassay systems assay (DIUR-500) according to the manufacturer's directions.

ATP Assay

Preweighed lung tissue was processed for determination of lung ATP content using commercially available reagents as per manufacturer's instructions (Abcam; ab833355). Briefly, frozen lung tissue was homogenized in ATP assay buffer using Dounce homogenizer. The lysate was centrifuged at 13,000 *g* at 4°C, and supernatant subjected to deproteinization procedure via TCA precipitation (Abcam; ab204708). The deproteinized samples were incubated with necessary reaction components for 30 min at room temperature protected from light. Fluorescence signals from samples were then measured on a microplate reader at Ex/Em = 535/587 nm. Serial dilutions of ATP were used to generate a standard calibration curve. ATP concentrations were calculated from the standard curve data and normalized to corresponding tissue weight.

Lung CXCL1

Lung CXCL1 was performed on whole lung homogenates by ELISA (R&D Systems, Minneapolis, MN) and corrected for protein (33). The detection limit is 1.0 pg/mL. Supernatants were analyzed for protein content using a Bio-Rad DC protein assay kit (Hercules, CA).

Lung Myeloperoxidase Activity

To determine myeloperoxidase (MPO) activity, lung tissue was homogenized in 1 mL of cold hexadecyltrimethylammonium bromide buffer, sonicated on ice for 10 s, and

centrifuged at 14,000 *g* for 30 min at 4°C. Twenty microliters of supernatant was transferred into a 96-well plate, and 200 μL of 37°. Odianisidine hydrochloride solution was added immediately before the optical density was read at 450 nm and again 30 s later, as previously described (37).

Statistical Analysis

Median fold change was determined for metabolites based on raw values (peak area) after metabolite identification comparing sham versus AKI for each time point. Then, metabolite intensities were autoscaled using MetaboAnalyst 5.0 (available at http://www.metaboanalyst.ca) to allow for homoscedastic statistical tests and to compare metabolites based on correlations. Univariate ANOVA was performed on autoscaled data followed by post hoc analysis with Sidak's multiple comparisons test (significant threshold for $P < 0.05$) using GraphPad Prism 9.0.0 comparing prespecified groups: normal versus all time points and sham versus AKI at identical time points (e.g., 24-h sham vs. 24-h AKI, but not 4-h sham vs. 24-h AKI). Principal component analysis was performed on all metabolites using Metaboanalyst 5.0 on all metabolites, and the first three principal components were analyzed. Hierarchical clustering analysis was performed on metabolites that were significant by ANOVA using Morpheus (https://software.broadinstitute.org/morpheus); the correlation metric used was the Pearson ($n - 1$) correlation with an average linkage method. Pathway enrichment analysis was performed using Metaboanalyst 5.0 (38) using Goeman's global test for the prespecified groups. A pathway was considered significant if the number of significant metabolite hits was 2 or more and the Holm-adjusted *P* value was less than 0.05.

ANOVA (using GraphPad Prism 9.0.0) was utilized to analyze serum creatinine and BUN, lung CXCL1, lung MPO activity, and lung ATP levels. Data were assessed for normality and distribution using the Shapiro-Wilk normality test and the Brown-Forsythe test, respectively. Normally distributed data were analyzed by one way ANOVA with Sidak correction for multiple comparison testing; for nonparametric data, the ANOVA was performed with the Kruskal–Wallis test and Dunn's correction for multiple comparison; for data with unequal variance, Welch ANOVA with Dunnett's correction for multiple comparison was performed.

RESULTS

Experimental Groups and Accounting for Mice Included in Experiments and Analysis

We began with 10 mice per group for each of the seven experimental groups: *1*) normal (no surgical procedure), *2*) 4-h sham, *3*) 4-h AKI, *4*) 24-h sham, *5*) 24-h AKI, *6*) 7-day sham, and *7*) 7-day AKI for a total of 70 mice. However, one mouse in the 7-day sham group died, and 4 mice in the 7-day AKI group died. Thus, the numbers of animals included in the final data analysis are as follows: *1*) normal: $n = 10$, *2*) 4-h sham: $n = 10$, *3*) 4-h AKI: $n = 10$, *4*) 24-h sham: $n = 10$, *5*) 24-h AKI: $n = 10$, *6*) 7-day sham: $n = 9$, and *7*) 7-day AKI: $n = 6$.

All of the data reported below were obtained from samples using this cohort of mice and can be found at the National Institute of Health's (NIH) Metabolomics Workbench (study ID: ST001747).

Time Course of Acute Kidney Injury, Lung Inflammation, and Lung Energy Production

To assess kidney function after AKI, serum creatinine and BUN were determined in normal mice and at 4 h, 24 h, and 7 days after sham and AKI procedures. As shown in Fig. 1*A*, serum creatinine was significantly increased at 4 and 24 h post AKI versus sham. There was no significant difference in serum creatinine at 7 days. BUN was significantly increased in AKI at all three time points (Fig. 1*B*). [The serum creatinine and BUN data in this cohort of mice has been previously published (34)]. We have previously demonstrated that this level of creatinine BUN rise is associated with histologic tubular injury (39) and loss of kidney function as judged by measured glomerular filtration rate (39). Although the BUN and creatinine are higher at 24 h versus 4 h, it is important to note that creatinine and BUN are not at steady state at the 4-h time point and the rate of rise lags behind the fall in kidney function; in fact, the loss of kidney function as determined by measured glomerular filtration rate is actually similar at 4 and 24 h after ischemic AKI (39, 40).

To assess lung inflammation after AKI, lung CXCL1 and MPO activity were determined in the same cohorts. As shown in Fig. 1, *C* and *D*, lung inflammation peaked at 4 h post-AKI: both lung CXCL1 and lung MPO activity were increased 4 h post-AKI with reduced levels at 24 h and 7 days. We have previously demonstrated the lung MPO activity correlates well with lung neutrophil accumulation as judged by flow cytometry (41) and histology (37). We have previously demonstrated that lung inflammation peaks by 4 h after AKI, and progressively declines at 24 h and 7 days (33, 42). Although there was drop-out due to mortality at 7 days post-AKI, the markers of lung inflammation (as well as kidney function) are similar to that observed 7 days post AKI in cohorts without significant mortality (42)—thus, it is expected that the findings in the lungs 7 days post-AKI in this cohort represent changes due to the aftereffects of AKI and not another confounding effect.

To assess lung energy production after AKI, lung ATP levels were determined in normal mice and at 4 h, 24 h, and 7 days after sham and AKI procedures. As shown in Fig. 2, lung ATP levels were significantly decreased 4 and 24 h after AKI versus sham at the same time point. There was no significant difference in lung ATP levels at 7 days. The group number is reduced for some groups due to sample loss from to repeated testing.

Metabolomics Analysis

Untargeted UHPLC-MS-based metabolomics analysis of the lung provided the measurement of 132 annotated metabolites as shown in Supplemental Table S1 (all Supplemental Material is available at https://doi.org/10.6084/m9.figshare.13299593).

To identify and visualize overall trends among experimental groups, principal component analysis (PCA) was performed on the autoscaled values (via Metaboanalyst) of these 132 metabolites. As shown in Fig. 3, PC1 largely illustrates the differences among replicates within each

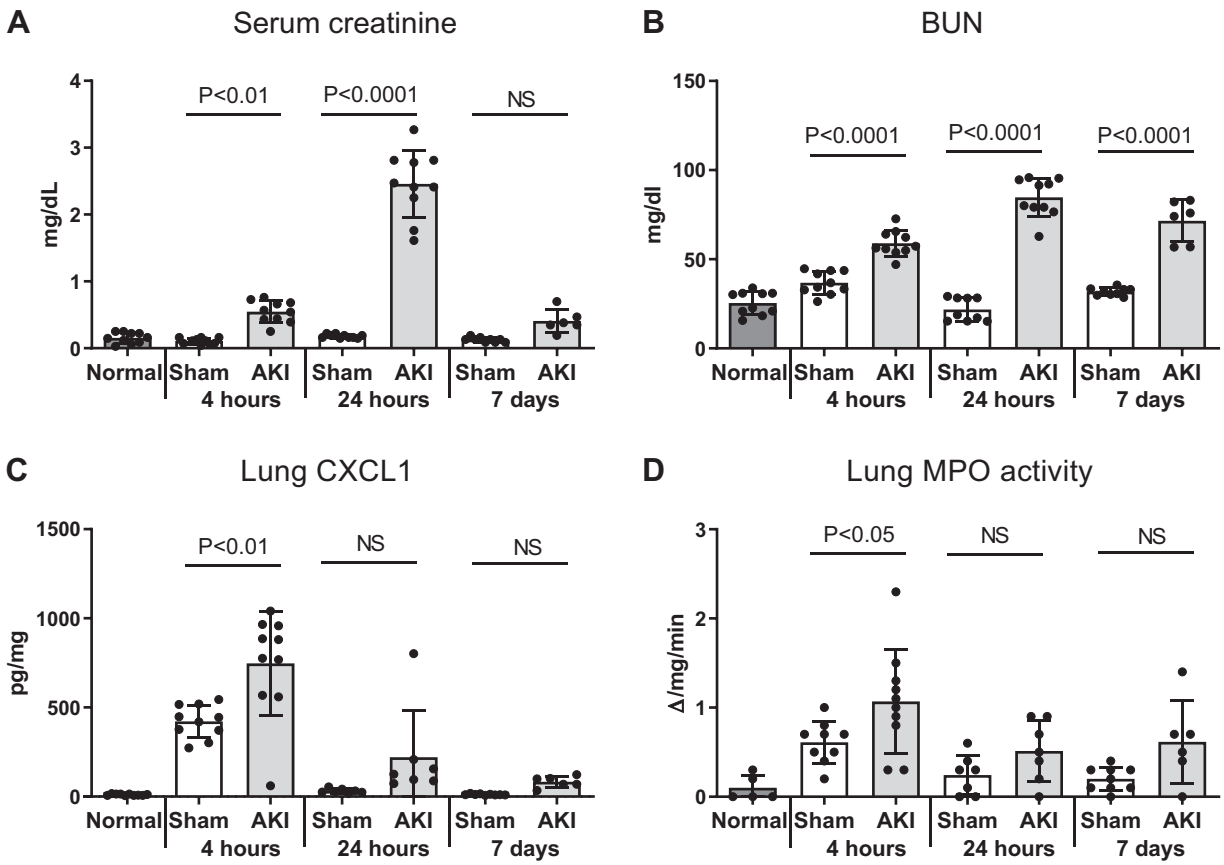

Figure 1. Time course of acute kidney injury and lung inflammation. Serum creatinine (*A*) and BUN (*B*) were determined in unmanipulated wild-type male mice ("Normal") and in wild-type male mice at 4 h, 24 h, and 7 days after surgery for Sham (surgery alone) and ischemic acute kidney injury (AKI). [The serum creatinine and BUN data from this cohort of mice have been previously published; 34)]. Lung CXCL1 (*C*) and lung MPO activity (*D*) were determined in normal controls and at 4 h, 24 h, and 7 days after Sham and AKI. Mean ± SD; one-way ANOVA comparing sham versus AKI at each time point. *n* represents number of mice. Normal: $n = 10$, 4-h Sham: $n = 10$, 4-h AKI: $n = 10$, 24-h sham: $n = 10$, 24-h AKI: $n = 10$, 7-day sham: $n = 9$, and 7-day AKI: $n = 6$. BUN, blood urea nitrogen; MPO, myeloperoxidase; NS, not significant.

biological group. Biological differences among groups are apparent via PC3 (9% variance) and PC2 (11.3% variance), illustrating the emergence of substantial differences in metabolic composition at 24 h post-AKI (sham in pink, AKI in yellow). At 7 days, the two groups cluster closer together (sham in red, AKI in green) though with a metabolic phenotype distinct from the other timepoints studied.

To further characterize the data set, univariate ANOVA (without post hoc testing) was performed for the 132 metabolites and 95 were found to be significantly different among experimental groups; these 95 metabolites are presented via hierarchical clustering analysis (HCA; Fig. 4). Broadly speaking, the HCA heat map demonstrates the following *1*) 4-h sham was associated with relative increases (identified in red) in numerous metabolites compared to the other groups, and *2*) 24-h AKI is characterized by metabolites that are both relatively decreased versus sham (in blue, upper portion of heat map) as well as increased versus sham (in red, lower portion of heat map).

With a global overview of the metabolic changes established, we next evaluated in detail the metabolic intermediates and pathways impacted by sham and AKI over time.

Effect of Sham and AKI on Individual Metabolite Levels

Sham versus normal.

Surgery, such as that performed in our sham cohort, is a physiologic stress that is expected to induce a specific metabolomic profile, as suggested by the HCA heat map demonstrating that 4-h sham was one of the most distinct groups. Therefore, to identify metabolites that were specifically affected by the surgical procedure itself, we compared the effect of sham at 4 h, 24 h, and 7 days to normal (ANOVA with Sidak post hoc correction). We observed the greatest sham effect at 4 h where 35 out of 95 metabolites (37%) were increased compared to normal, consistent with the results from the HCA analysis. Of these metabolites, 18 participate in amino acid metabolism suggestive of a catabolic state, shifting sources of energy, or increased protein synthesis; 12 are involved in energy production (glycolysis, TCA cycle, pentose phosphate pathway and purine/pyrimidine metabolism); and three are involved in oxidative stress regulation. Five metabolites were increased at 24 h, and five were increased at 7 days (Supplemental Table S2).

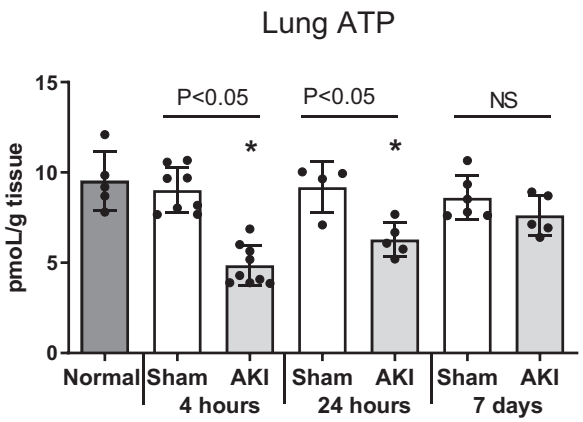

Figure 2. ATP levels are reduced in the lung at 4 and 24 h after acute kidney injury (AKI). ATP levels were determined in the lung in unmanipulated wild-type male mice ("Normal") and in wild-type male mice at 4 h, 24 h, and 7 days after surgery for Sham (surgery alone) and ischemic acute kidney injury. Mean ± SD; one-way ANOVA comparing Sham versus AKI at each time point, and all groups vs. normal; $*P < 0.05$ vs. Normal. *n* represents number of mice. Normal: $n = 5$, 4-h Sham: $n = 8$, 4-h AKI: $n = 9$, 24-h Sham: $n = 4$, 24-h AKI: $n = 5$, 7-day Sham: $n = 6$, and 7-day AKI: $n = 5$. NS, not significant.

AKI versus normal.

To identify metabolites affected by AKI relative to normal, we compared the effect of 4-h, 24-h, and 7-day AKI versus normal (ANOVA with Sidak post hoc correction). We determined 48 metabolites out of 95 that were increased in AKI versus normal. Thirteen of those were increased 4 h after AKI versus normal. We observed the greatest AKI affect at 24 h where 20 of the 48 metabolites were increased compared to normal. At 7 days, 15 of 48 metabolites were increased (Supplemental Table S3).

4-h sham and 4-h AKI.

Since 4-h sham demonstrated numerous metabolite differences that were not observed 4 h after AKI, we sought to better visualize and characterize the changes between sham and AKI at this time point. As shown in Supplemental Fig. S1, of the 35 metabolites that were significantly increased 4 h after sham versus normal, only 11 were also increased 4 h after AKI versus normal. Since lung ATP levels were normal 4 h after sham and reduced 4 h after AKI, we conclude that the increase in metabolites 4 h after sham is an appropriate metabolic response after surgical stress that is impaired during AKI.

Sham versus AKI, Time Course of Metabolite Changes in the Lung

To further assess whether the metabolic response to surgical stress after AKI is appropriate and assess this effect over time the following groups were compared: *1*) 4-h sham versus 4-h AKI, *2*) 24-h sham versus 24-h AKI, and *3*) 7-day sham versus 7-day AKI (by ANOVA with Sidak post hoc correction). Normalized values for significant metabolites are presented in Figs. 5–9. The metabolites are grouped into the following broad ontologies: antioxidants (e.g., glutathione) and metabolites involved in the oxidative stress response (Fig. 5); amino acid and related metabolites (Figs. 6 and 7); energy related metabolites which include carbohydrates and related carbohydrate alcohols (Fig. 8) and purine and pyrimidine metabolites (Fig. 9). Tables 1 and 2 offer a tabulated version of metabolite changes in AKI versus sham as arranged by time: 4 h, 24 h, and 7 days. Below we describe the analytes and relative changes in the patterns of each ontological group over time.

Increased Oxidative Stress in AKI

Evidence of increased oxidative stress was present after AKI as judged by significantly reduced levels of the antioxidants glutathione and thioredoxin disulfide 24 h after AKI. Furthermore, numerous metabolites involved in glutathione metabolism and synthesis were reduced after AKI (Fig. 5). Specifically, glutamate (Fig. 6), Cys-Gly (Figs. 5 and 6), and glutathione disulfide (Fig. 5) were lower in AKI levels compared to sham. 5-Oxoproline, gamma-L-glutamyl-D-alanine, and 5-L-glutamyl-glutamine (Fig. 6), demonstrated similar reduced metabolite trends compared to sham but did not reach statistical significance.

Alternative Energy Production

As in other tissues, oxidative phosphorylation is the predominant and preferred pathway for energy production in the lung. Numerous stresses and injuries may interfere with or inhibit oxidative phosphorylation, requiring alternative sources of energy production (e.g., anerobic glycolysis, purine metabolism). In addition, alternative mechanisms of energy metabolism may need to be employed to support ongoing oxidative phosphorylation (e.g., anaplerosis to replenish TCA cycle intermediates). As shown in Figs. 6–9,

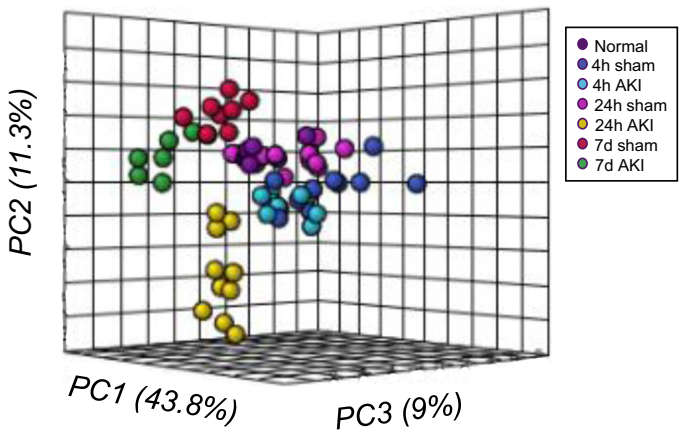

Figure 3. Differential lung metabolic phenotypes represented by principal component analysis. Metabolites (132) were identified in the lung following untargeted UHPLC-MS-based metabolomics analysis in unmanipulated wild-type male mice ("Normal") and in wild-type male mice at 4 h, 24 h, and 7 days after surgery for Sham (surgery alone) and ischemic acute kidney injury (AKI). Principal component analysis was performed on these metabolites using the Pearson ($n - 1$) correlation following autoscaling of the raw data in MetaboAnalyst 5.0. PC1 largely illustrates the differences among replicates within each biological group. Biological differences among groups are apparent via PC3 (9% variance) and PC2 (11.3% variance), illustrating the emergence of substantial differences in metabolic composition at 24 h post-AKI (sham in pink, AKI in yellow). At 7 days, the two groups cluster closer together (sham in red, AKI in green) though with a metabolic phenotype distinct from the other time points studied. *n* represents number of mice. Normal: $n = 5$, 4-h sham: $n = 8$, 4-h AKI: $n = 9$, 24-h sham: $n = 4$, 24-h AKI: $n = 5$, 7-day sham: $n = 6$, and 7-day AKI: $n = 5$. PC, principal component; UHPLC-MS, ultra-high-pressure liquid chromatography coupled to online mass spectrometry.

AJP-Lung Cell Mol Physiol • doi:10.1152/ajplung.00042.2020 • www.ajplung.org

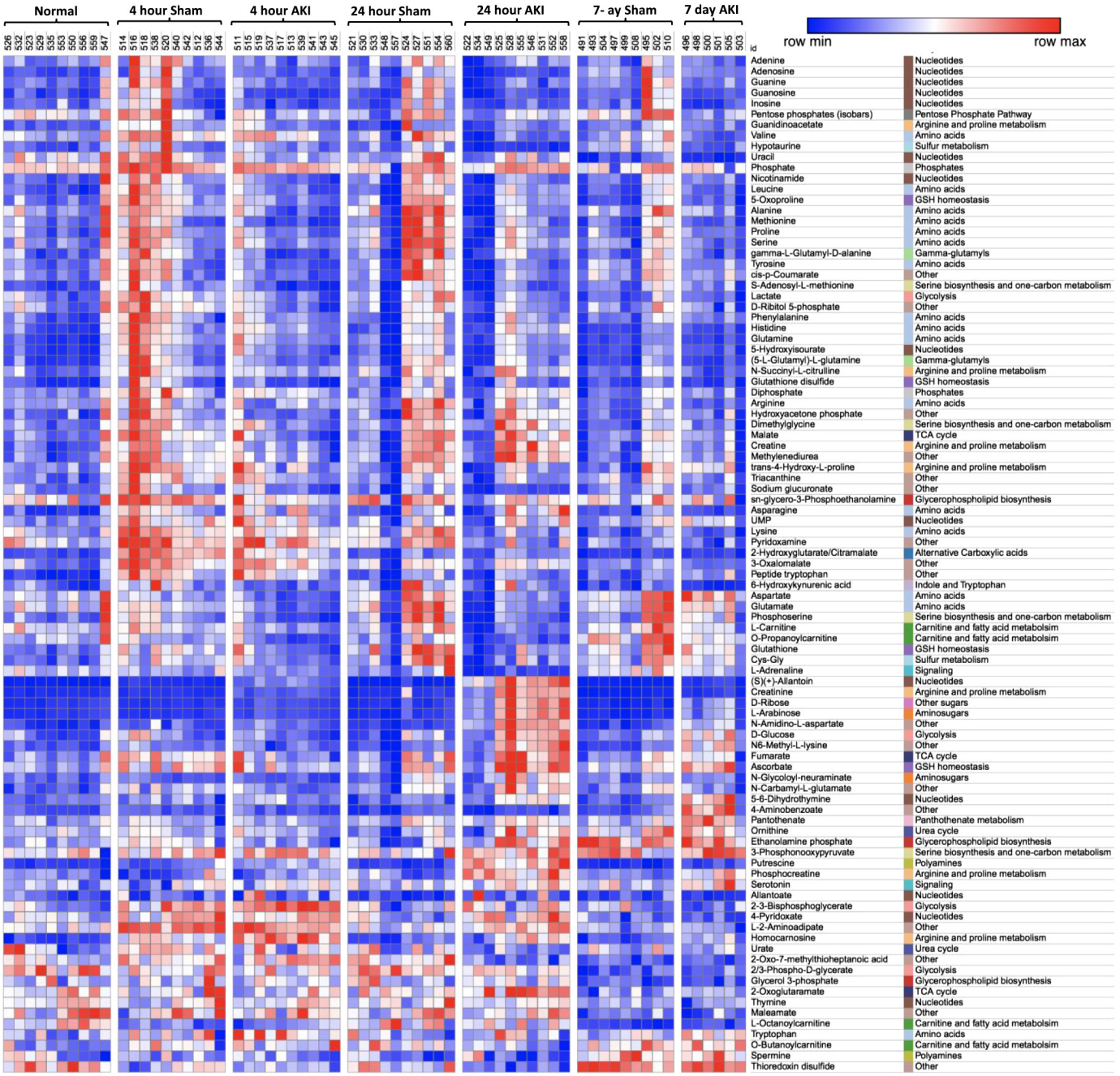

Figure 4. Hierarchical clustering analysis (HCA) of lung metabolites. HCA, with predefined sample clusters, was performed for the 95 lung metabolites that were significantly different among groups as judged by ANOVA (without post hoc testing) to determine trends for individual metabolites among experimental groups. Each column cluster represents an experimental cohort as labeled (Normal, 4-h sham, 4-h AKI, 24-h sham, 24 -h AKI, 7-day sham, and 7-day AKI), whereas each individual column represents an experimental mouse subject (Normal: $n = 10$, 4-h sham: $n = 10$, 4-h AKI: $n = 10$, 24-h sham: $n = 10$, 24-h AKI: $n = 10$, 7-day sham: $n = 9$, and 7-day AKI: $n = 6$). Each row represents a metabolite. To the right of each row is the corresponding metabolite name and general category. Red represents increasing metabolites whereas blue represents decreasing metabolites. The correlation metric used was the Pearson ($n - 1$) correlation with an average linkage method. Two major effects are observed: *1*) 4-h sham is associated with relative increases (identified in red) of numerous metabolites compared to the other groups, and *2*) 24-h AKI is characterized by metabolites that are both relatively decreased versus sham (in blue, upper portion of heat map) as well as increased versus sham (in red, lower portion of heat map). AKI, acute kidney injury.

changes in metabolite levels suggest that AKI is associated with numerous alternative mechanisms of energy production including increased amino acid metabolism and anaplerosis; energy shifts associated with glycolysis, the TCA cycle and pentose phosphate pathway; and increased nucleotide metabolism.

Alternative Energy Production: Amino Acid Catabolism

At all time points, we observed altered levels of amino acids and their metabolites. We interpret these findings as evidence of increased metabolism and/or upregulated anaplerotic activity to maintain ATP production through replenishing TCA

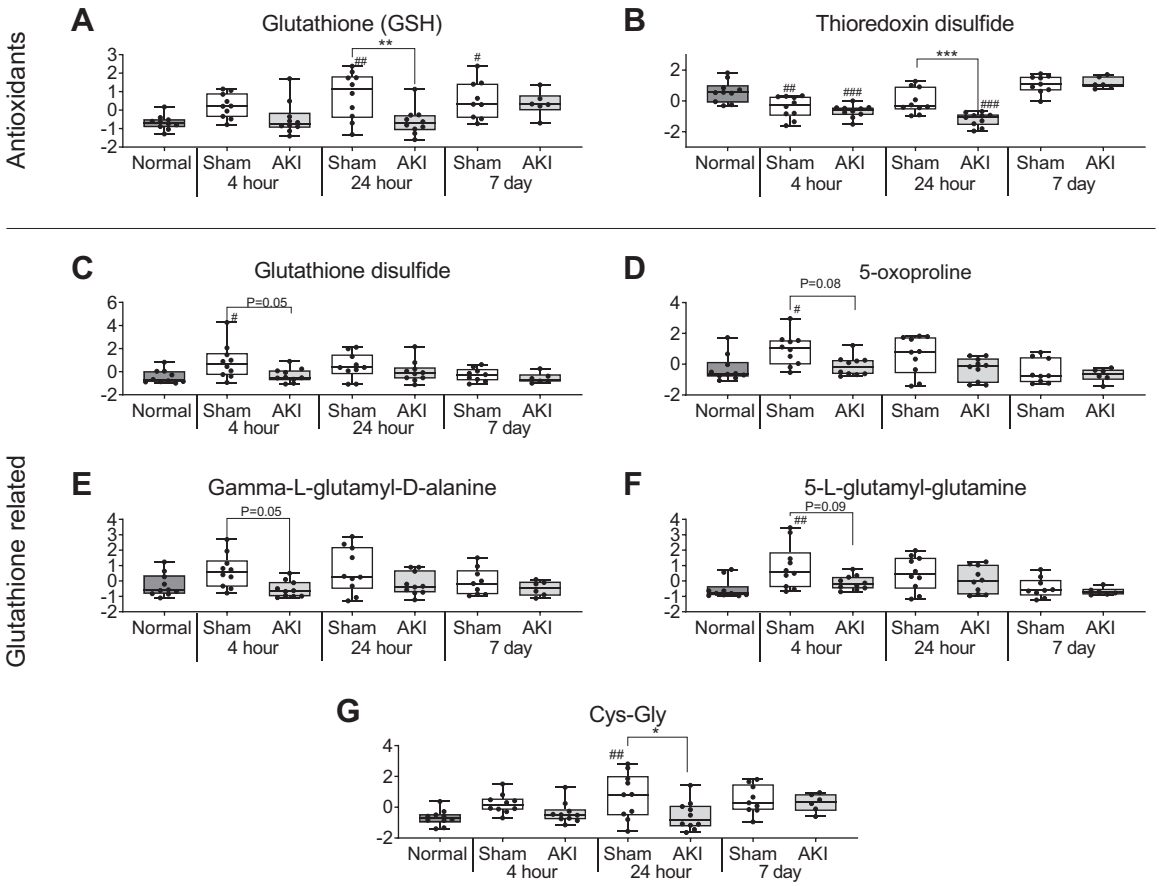

Figure 5. Metabolites involved in oxidative stress affected in the lung following acute lung injury (AKI). The antioxidants glutathione (*A*) and thioredoxin (*B*) and several metabolites involved in glutathione synthesis (*C*–*G*) were reduced in the lung at 4 h or 24 h after AKI, suggesting the presence of increased oxidative stress. Data are metabolites detected by untargeted UHPLC-MS-based metabolomics analysis that were determined in unmanipulated male wild-type mice ("Normal") and in wild-type male mice at 4 h, 24 h, and 7 days after surgery for sham (surgery alone) and ischemic acute kidney injury. Data were normalized via autoscaling and are presented as box and whisker plots which show individual data points, the median and the 25th and 75th percentiles as the "boxes," and the min and max values as the "whiskers." One-way ANOVA comparing Sham versus AKI at each time point, and all groups vs. Normal; $^{**}P < 0.01$, $^{***}P < 0.001$; $^{\#}P < 0.05$ vs. Normal, $^{\#\#}P < 0.01$ vs. Normal, $^{\#\#\#}P < 0.001$ vs. Normal. *n* represents number of mice. Normal: $n = 10$, 4-h sham: $n = 10$, 4-h AKI: $n = 10$, 24-h sham: $n = 10$, 24-h AKI: $n = 10$, 7-day sham: $n = 9$, and 7-day AKI: $n = 6$. UHPLC-MS, ultra-high-pressure liquid chromatography coupled to online mass spectrometry.

cycle intermediates and supporting oxidative phosphorylation. At 4 h, homocarnosine was increased and S-adenosyl-L-methionine was decreased, both are associated with amino acid catabolism.

Strikingly, 18 of the 30 significant metabolites at 24 h compared to sham were amino acids or amino acid derivatives (Tables 1 and 2). Of those, 11 were decreased compared to sham at 24 h (Figs. 6 and 7), including amino acids lysine, alanine, aspartate, valine and glutamate (also a glutathione precursor), and amino acid metabolites Cys-Gly (also a glutathione precursor), phosphoserine, adrenaline, carnitine, propanoylcarnitine, and hypotaurine.

Conversely, seven amino acid metabolites were increased at 24 h in AKI compared to sham. This included 2-aminoapidate, homocarnosine, putrescine, *N*-6-methyl-lysine, and *N*-amidino-L-aspartate. Specifically, alterations in 2-aminoapidate and *N*-6-methyl-lysine, coupled with reduced lysine metabolite levels, suggests lysine catabolism, which yields CoA and glutamate available to enter the TCA cycle. Increased levels of *N*-amidino-L-aspartate, homocarnosine and putrescine are representative of protein catabolism.

At 7 days, the amino acid metabolite *N*-6-methyl-L-lysine was increased.

Alternative Energy Production: Glycolysis, TCA, and PPP

Additional support for the upregulation of alternative and supplemental energy metabolism was evidenced by metabolite alterations in glycolysis, TCA and PPP pathways.

At 4 h, 2-hydroxyglutarate/citralamate and malate (TCA cycle), lactate (glycolysis), D-ribitol-5-phosphate (PPP) were reduced.

At 24 h, upregulation of alternate sources of ATP were evidenced by increased levels of D-glucose (intermediate in glycolysis) and D-ribose and L-arabinose (intermediates in PPP). Vitamin B6 is an essential cofactor in multiple energy-related reactions. Two vitamin B6 metabolites were altered at 24 h compared to sham. Specifically, 4-pyridoxate (pyridoxic acid) was increased, and pyridoxamine was decreased. Higher pyridoxic acid and lower pyridoxamine measurements are indicative of vitamin B6 catabolism.

AJP-Lung Cell Mol Physiol • doi:10.1152/ajplung.00042.2020 • www.ajplung.org

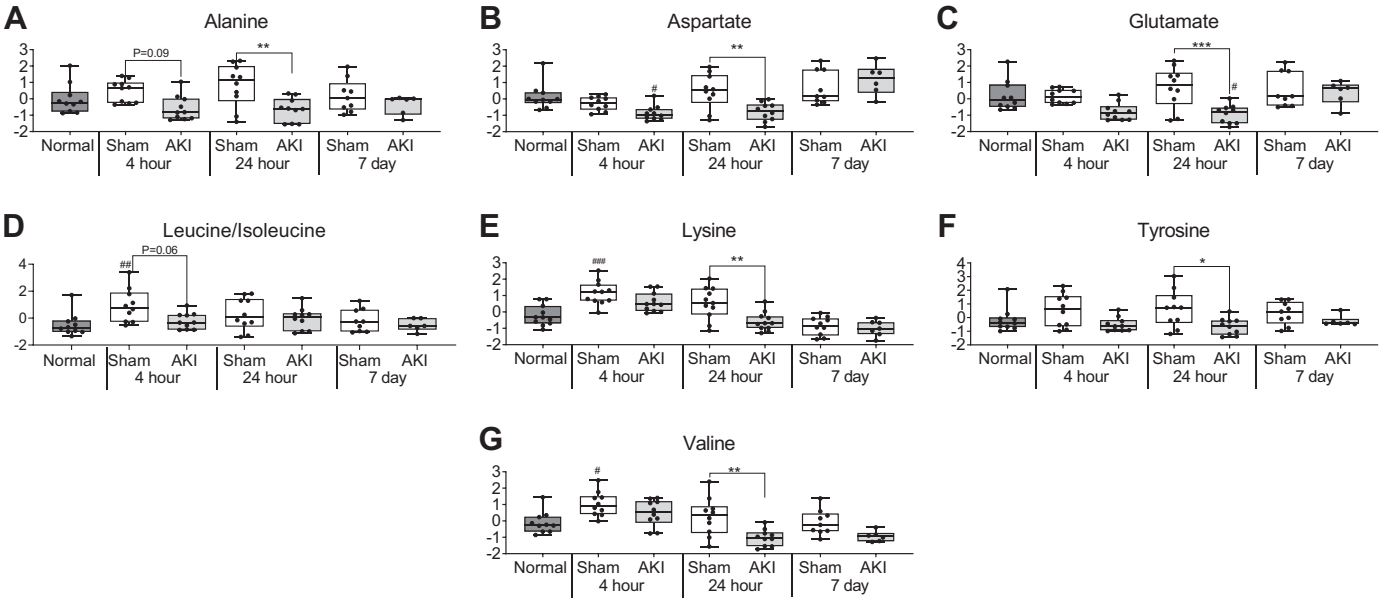

Figure 6. Amino acids affected in the lung after acute kidney injury (AKI). Seven amino acids (*A*–*G*) were reduced in the lung at 4 and/or 24 h after AKI, suggesting the presence of amino acid consumption. Data are metabolites detected by untargeted UHPLC-MS-based metabolomics analysis that were determined in unmanipulated male wild-type mice ("Normal") and in wild-type male mice at 4 h, 24 h, and 7 days after surgery for Sham (surgery alone) and ischemic acute kidney injury. Data were normalized via autoscaling and are presented as box and whisker plots which show individual data points, the median and the 25th and 75th percentiles as the "boxes," and the min and max values as the "whiskers." One-way ANOVA comparing Sham versus AKI at each time point, and all groups vs. Normal; $^{*}P < 0.05$, $^{**}P < 0.01$, $^{***}P < 0.001$; $^{\#}P < 0.05$ vs. Normal, $^{\#\#}P < 0.01$ vs. Normal, $^{\#\#\#}P < 0.001$ vs. Normal. *n* represents number of mice. Normal: $n = 10$, 4-h sham: $n = 10$, 4-h AKI: $n = 10$, 24-h sham: $n = 10$, 24-h AKI: $n = 10$, 7-day sham: $n = 9$, and 7-day AKI: $n = 6$. UHPLC-MS, ultra-high-pressure liquid chromatography coupled to online mass spectrometry.

At 7 days, D-ribose and L-arabinose (PPP metabolites) and pantothenate (vitamin B5 metabolite essential in synthesis of CoA for TCA cycle) were increased.

Alternative Energy Production: Nucleotide Metabolism

Nucleotide metabolism can be associated with ATP depletion and efforts to replenish it through alternate routes. At 4 and 24 h, allantoin, an end product of purine metabolism and known marker of oxidative stress, was increased. Additionally, known constituents of ATP, adenine and adenosine, were decreased at 4 h. We interpret decreased adenine and adenosine values to be evidence of their depletion due to ATP regeneration. Finally, 5, 6-dihydrothymine (a pyrimidine metabolite) was increased at 24 h and 7 days compared to sham.

Pathway Analysis

In further support of upregulated utilization of alternative energy sources, pathway analysis demonstrated PPP enrichment at all time points in AKI compared to sham. Lysine degradation pathways, supportive of anaplerotic reactions for upregulated TCA activity, were enriched at 24 h. Finally, starch and sucrose metabolism were enriched 7 days post AKI (Table 3).

Comparison of Lung Metabolic Findings to the Kidney, Plasma, and Heart

Metabolite analysis of kidney, plasma, and heart from this cohort was previously determined and those data have been published (34). Therefore, we assessed whether there were similarities between the metabolomics findings in the lung compared to the kidney, plasma, or heart. Globally, there were some similarities and evidence of increased oxidative stress and a shift to alternative energy production were also present in the kidney, plasma, and heart. That said, the derangements in specific metabolites had minimal overlap, as shown in Supplemental Tables S4–S7 in which significantly changed metabolites in the lung, kidney, plasma, and heart are compared. As an example, 24 h after AKI, 24 metabolites were increased in the heart and 14 were increased in the lung, but only five of these metabolites were common to both organs. Thus, although AKI is associated with global systemic metabolic effects that are similar among organs, the metabolic phenotype of each organ is distinct.

DISCUSSION

Clinically, AKI is associated with numerous respiratory complications that includes increased risk of respiratory failure requiring mechanical ventilation and prolonged weaning (10). Animal models of AKI have provided substantial insight into the effects of AKI on the lungs and demonstrated that AKI-mediated lung injury is characterized by lung inflammation, apoptosis, increased capillary leak, and dysregulation of salt and water channels (10). To date, however, the effect of AKI on oxidative stress, metabolism, and energy production had not been examined. In the present report, we performed lung metabolomics assessment and examined lung energy production after ischemic AKI in mice. Numerous novel findings regarding the effect of AKI on the lung were observed including *1*) increased oxidative stress, *2*) evidence of a shift toward alternate methods of energy production, and *3*)

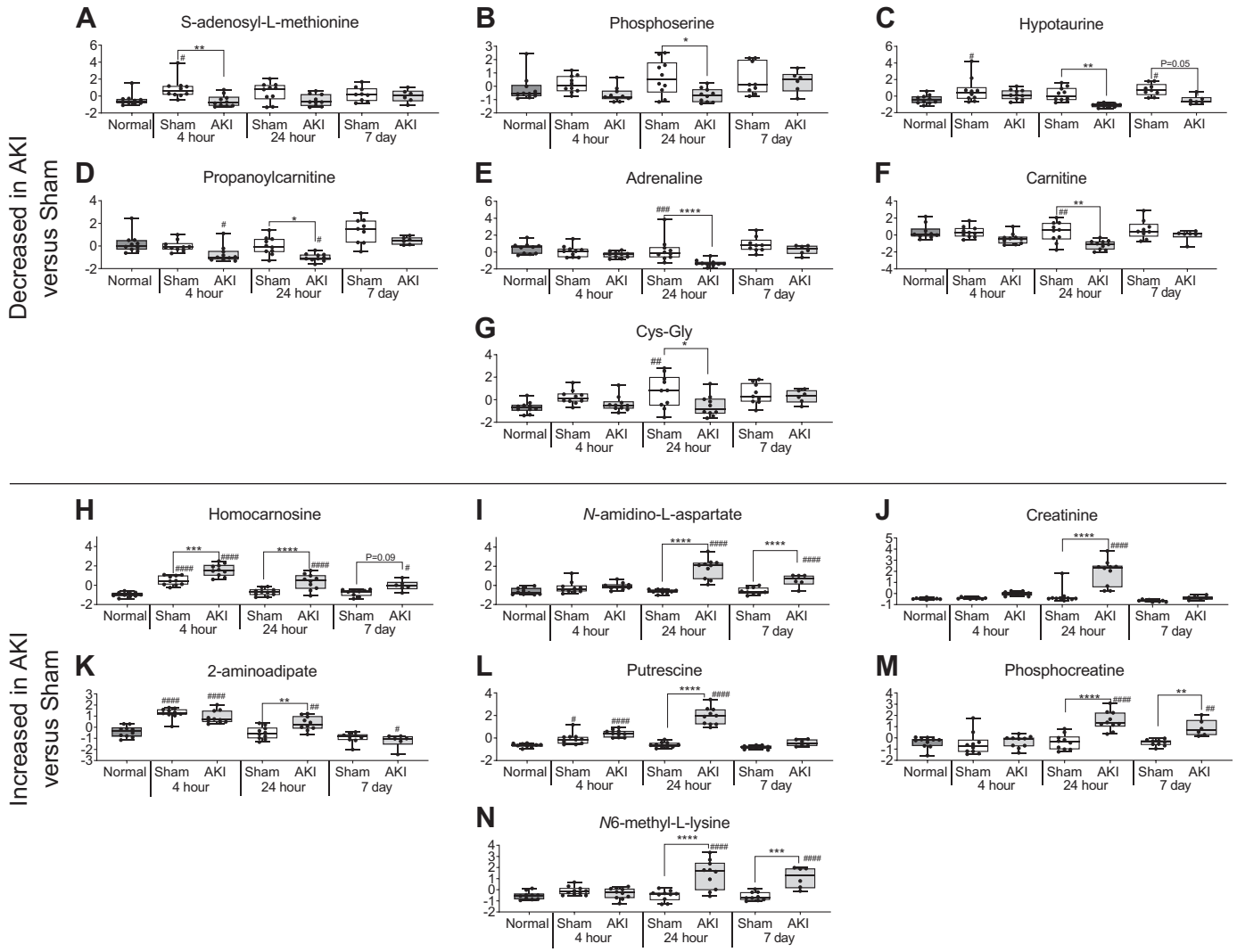

Figure 7. Amino acid metabolites affected in the lung after acute kidney injury (AKI). 14 amino acid-related metabolites (*A*–*N*) were affected in the lung at 4 h, 24 h, and/or 7 days after sham or AKI. Some metabolites were decreased after AKI (*A*–*G*) and some were increased after AKI (*H*–*N*). Data are metabolites detected by untargeted UHPLC-MS-based metabolomics analysis that were determined in unmanipulated male wild-type mice ("Normal") and in wild-type male mice at 4 h, 24 h, and 7 days after surgery for sham (surgery alone) and ischemic acute kidney injury. Data were normalized via autoscaling and are presented as box and whisker plots which show individual data points, the median and the 25th and 75th percentiles as the "boxes," and the min and max values as the "whiskers." One-way ANOVA comparing sham versus AKI at each time point, and all groups vs. Normal; $^{*}P < 0.05$, $^{**}P < 0.01$, $^{***}P < 0.001$, $^{****}P < 0.0001$; $^{\#}P < 0.05$ vs. Normal, $^{\#\#}P < 0.01$ vs. Normal, $^{\#\#\#}P < 0.001$ vs. Normal, $^{\#\#\#\#}P < 0.0001$ vs. Normal. *n* represents number of mice. Normal: $n = 10$, 4-h Sham: $n = 10$, 4-h AKI: $n = 10$, 24-h sham: $n = 10$, 24-h AKI: $n = 10$, 7-day sham: $n = 9$, and 7-day AKI: $n = 6$. UHPLC-MS, ultra-high-pressure liquid chromatography coupled to online mass spectrometry.

depleted levels of ATP. The findings in this report bring to light novel characteristics of AKI-mediated lung injury, provide new leads into the mechanisms by which AKI in patients predisposes to pulmonary complications, and lend additional insight into the complex systemic nature of AKI in general.

The effects of AKI on the lungs have been widely studied in animal models (8, 43, 44) and like other causes of indirect lung injury, AKI-mediated lung injury is associated with lung inflammation and characterized by increased levels of lung cytokines, chemokines, and neutrophils (33, 37, 45, 46) that are present by 4 h post-AKI. 24 h after AKI, T cell accumulation (47) and various forms of cell death including necroptosis (48), parthanatos (48), and apoptosis (49) are present. In the present study, the inflammatory nature of lung injury after AKI was confirmed by assessing levels of the neutrophil chemokine CXCL1 as well as lung MPO activity (a marker of lung neutrophils) which were increased by 4 h post-AKI. Unlike models of direct lung injury, AKI-mediated lung injury is not characterized by significant epithelial injury and the alveolar space (as judged by histology and analysis of BAL fluid) is relatively devoid of inflammatory cytokines and neutrophils, which is similar to other indirect models of lung injury; pulmonary edema is generally present, and elevated levels of BAL fluid protein are variably reported.

Whether the increased oxidative stress, changes in energy metabolism, and reduced ATP production observed in the present study are due to the inflammatory nature of AKI-mediated lung injury is unresolved. A variety of models of lung inflammation are also associated with increased oxidative stress and reduced ATP levels and includes the direct

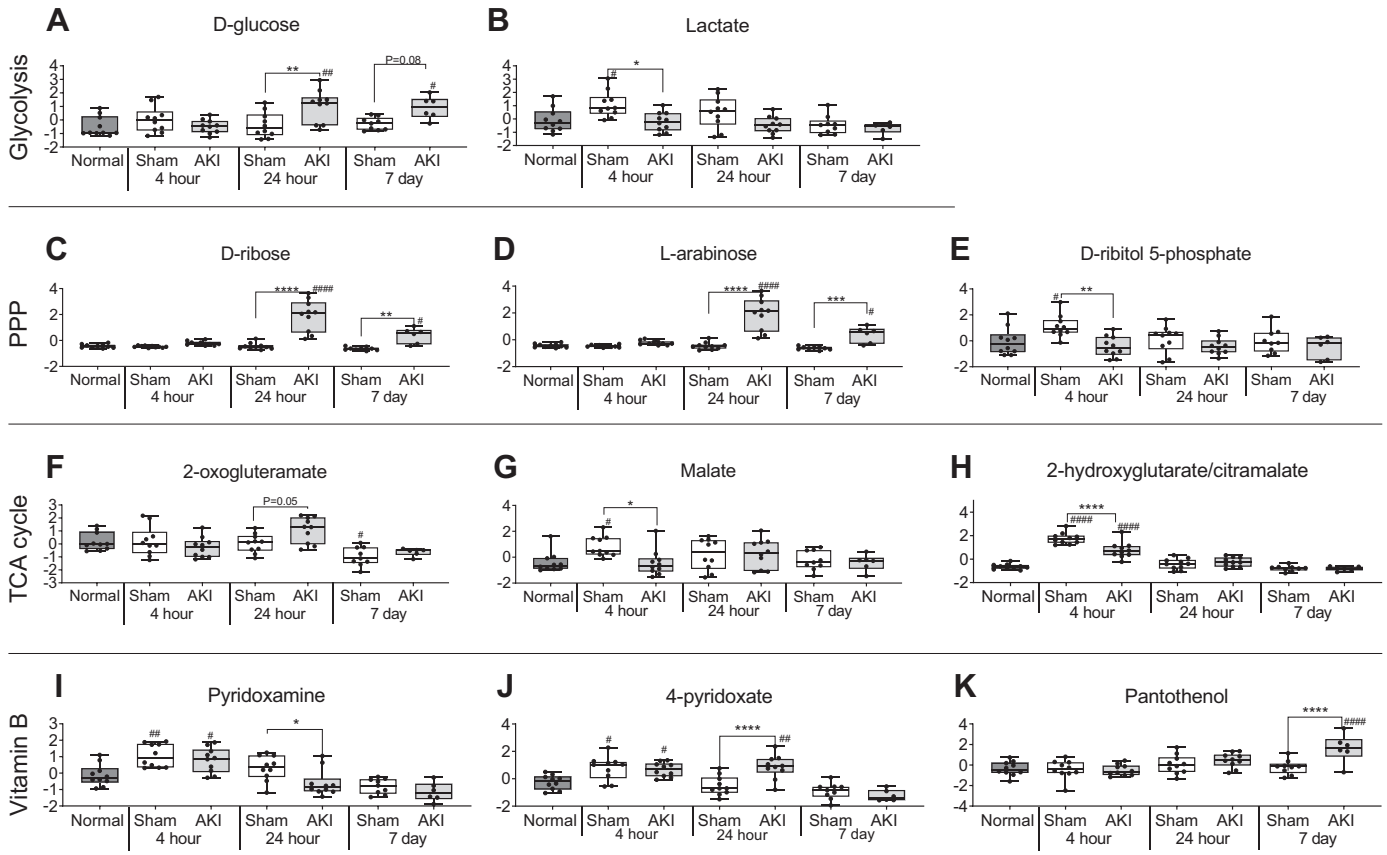

Figure 8. Energy metabolites are affected in the lung after acute kidney injury (AKI). Metabolites involved in glycolysis (*A* and *B*), pentose phosphate pathway (PPP) (*C–E*), the TCA cycle (*F–H*), and vitamin B metabolism (*I–K*) were affected in the lung at 4 h, 24 h, and/or 7 days after sham and/or AKI in the lung. Data are metabolites detected by untargeted UHPLC-MS-based metabolomics analysis that were determined in unmanipulated male wild-type mice ("Normal") and in wild-type male mice at 4 h, 24 h, and 7 days after surgery for sham (surgery alone) and ischemic acute kidney injury. Data were normalized via autoscaling and are presented as box and whisker plots which show individual data points, the median and the 25th and 75th percentiles as the "boxes," and the min and max values as the "whiskers." One-way ANOVA comparing Sham versus AKI at each time point, and all groups vs. Normal; $^{*}P < 0.05$, $^{**}P < 0.01$, $^{***}P < 0.001$, $^{****}P < 0.0001$; $^{\#}P < 0.05$ vs. Normal, $^{\#\#}P < 0.01$ vs. Normal, $^{\#\#\#\#}P < 0.0001$ vs. Normal. *n* represents number of mice. Normal: $n = 10$, 4-h sham: $n = 10$, 4-h AKI: $n = 10$, 24-h sham: $n = 10$, 24-h AKI: $n = 10$, 7-day sham: $n = 9$, and 7-day AKI: $n = 6$. UHPLC-MS; ultra-high-pressure liquid chromatography coupled to online mass spectrometry.

injury models of intratracheal (IT) TNF-α, IT lipopolysaccharide (LPS), influenza, cigarette, and smoke exposure and indirect models of sepsis (e.g., cecal ligation and puncture), intraperitoneal LPS, and intestinal ischemia reperfusion injury. Since neutrophil accumulation and activation is a major source of ROS and ROS accumulation can directly inhibit mitochondrial function (50), future investigation of the role of neutrophil accumulation on ROS, energy metabolism, and ATP production levels merits investigation.

AKI is associated with an increase in numerous circulating factors which could potentially play a role in affecting lung energy metabolism. In particular, we have demonstrated that the proinflammatory cytokine IL-6 is a major mediator of lung inflammation post-AKI. The rise in IL-6 post-AKI is multifactorial and related to surgical stress, increased renal and extra-renal production, increased production by macrophages, and decreased renal clearance (51, 52).

IL-6 is increased in the plasma as early as 2 h after AKI in patients (11) and mice (37) and methods to inhibit IL-6 in murine models result in reduced lung inflammation post-AKI (41, 53). Specifically, we have shown that IL-6 mediates upregulation of the neutrophil chemokine CXCL1 which promotes lung neutrophil accumulation; methods to inhibit IL-6 are associated with reduced lung CXCL1 and lung neutrophils (33); inhibition of CXCL1 function using CXCR2-deficient mice and anti-CXCL1 antibodies protected against lung neutrophil accumulation (54), highlighting the role of CXCL1 in mediating lung inflammation after AKI (CXCR2 is a receptor for CXCL1). In addition to its role in mediating inflammation, IL-6 plays a role in energy metabolism by promoting glucose metabolism (55). Other systemic consequences of AKI besides proinflammatory effects might explain the change in energy metabolism post-AKI. Although not assessed, tubular injury and necrosis associated with renal ischemia reperfusion leads to the elaboration and release of numerous danger-associated molecular patterns (DAMPs) such as histones which are known mediators of AKI-induced lung injury (48). In addition, AKI is characterized by the accumulation of numerous metabolites and uremic toxins which could potentially have deleterious effects on lung energy metabolism.

In a previously published study, we reported the metabolomics findings in this same cohort of mice in the kidney, plasma, and heart (34) and found evidence of increased oxidative stress, and evidence of alternative energy production

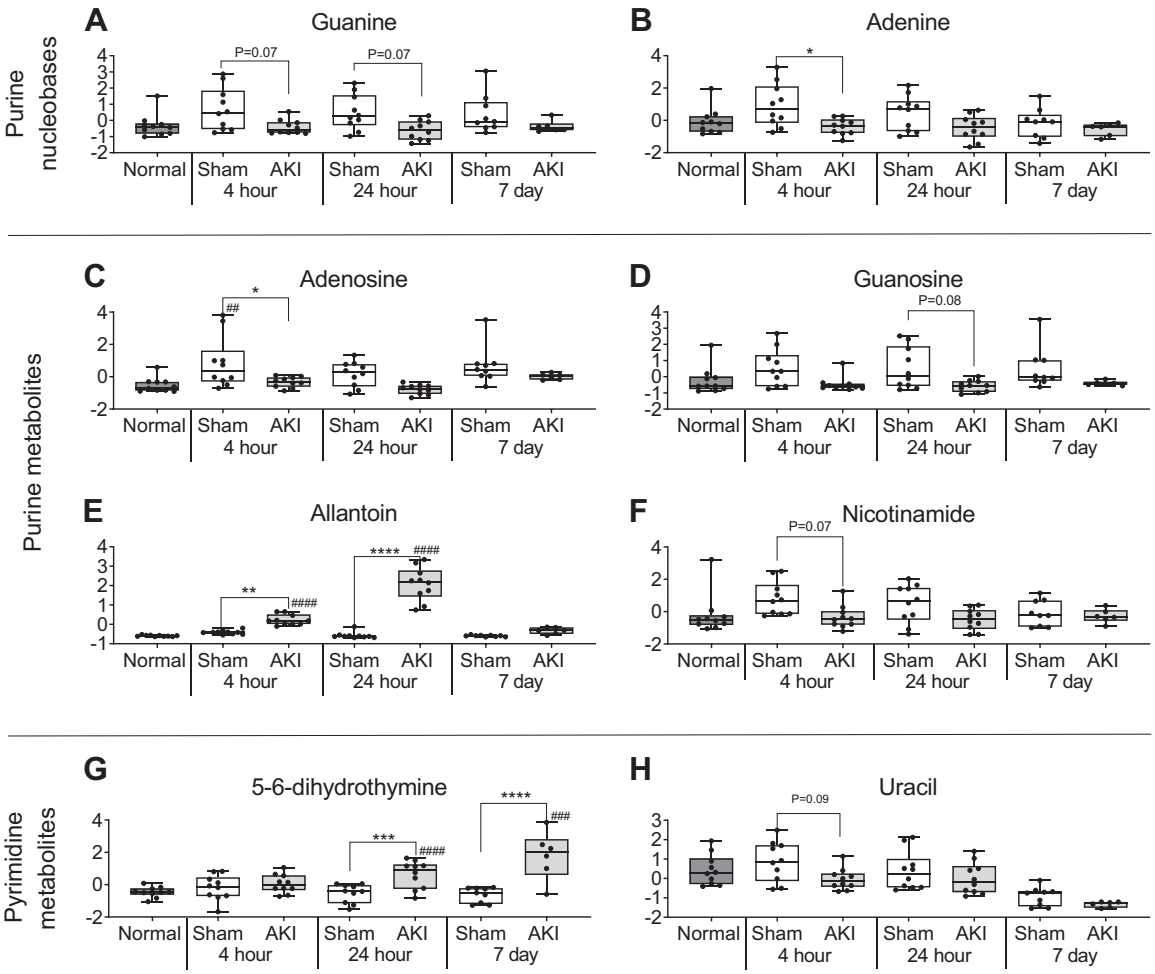

Figure 9. Purine and pyrimidine metabolites are affected in the lung after acute kidney injury (AKI). Metabolites involved in purine and pyrimidine metabolism including the purine nucleobases guanine (*A*) and adenine (*B*), purine metabolites (*C*–*F*), and pyrimidine metabolites (*G* and *H*) were affected in the lung at 4 h, 24 h, and/or 7 days after sham and/or AKI. Data are metabolites detected by untargeted UHPLC-MS-based metabolomics analysis that were determined in unmanipulated male wild-type mice ("Normal") and in wild-type male mice at 4 h, 24 h, and 7 days after surgery for Sham (surgery alone) and ischemic acute kidney injury. Data were normalized via autoscaling and are presented as box and whisker plots which show individual data points, the median and the 25th and 75th percentiles as the "boxes," and the min and max values as the "whiskers." One-way ANOVA comparing Sham versus AKI at each time point, and all groups vs. Normal; $^{*}P < 0.05$, $^{**}P < 0.01$, $^{***}P < 0.001$, $^{****}P < 0.0001$; $^{\#\#}P < 0.01$ vs. Normal, $^{\#\#\#}P < 0.001$ vs. Normal, $^{\#\#\#\#}P < 0.0001$ vs. Normal. *n* represents number of mice. Normal: $n = 10$, 4-h sham: $n = 10$, 4-h AKI: $n = 10$, 24-h sham: $n = 10$, 24-h AKI: $n = 10$, 7-day sham: $n = 9$, and 7-day AKI: $n = 6$. UHPLC-MS, ultra-high-pressure liquid chromatography coupled to online mass spectrometry.

in the kidney, plasma, and heart. Notably, amino acid deficiency was present in all three compartments, and lower levels of glutathione were noted in the plasma and heart; in the present study, we found that certain amino acids and glutathione were also reduced in the lung. Lower levels of ATP were also noted in the heart after AKI. Thus, it is possible that energy substrate deficiency and increased oxidative stress lead to impaired ATP production in both the lung and heart after AKI. Regardless of the cause, it may be said that AKI is systemically associated with increased oxidative stress, amino acid depletion, and altered energy production which is associated with reduced levels of ATP in both the heart and lung. Of note, even though certain overall changes in energy metabolism were similar between the heart and lung, it is important to note the specific changes in metabolites in these organs was distinct, thus highlighting the complex systemic effects of AKI in general, and on energy metabolism in particular.

In the present study, the evidence of increased oxidative stress in the lung after AKI was most notably apparent with regard to the lower levels of cellular glutathione pools. Glutathione depletion is a hallmark of increased oxidative stress. As a potent ROS scavenger, glutathione is critically important in normal lung homeostasis and protection against ROS mediated lung injury. Whether glutathione depletion is a result of increased glutathione utilization (e.g., glutathionylation of proteins, which is used as a mechanism to protect redox sensitive protein cysteine from being irreversibly overoxidized) or impaired synthesis or another mechanism is unknown, and a future line of investigation. Regardless of cause, glutathione depletion is a well-described consequence of numerous lung injuries that includes sepsis, IT LPS, cigarette smoke, and infections. In patients, lung glutathione depletion has been associated with increased susceptibility to and severity of ARDS. For example, patients who chronically abuse alcohol have reduced levels of lung glutathione and have both increased incidence

AJP-Lung Cell Mol Physiol • doi:10.1152/ajplung.00042.2020 • www.ajplung.org

Table 1. *Metabolites decreased in AKI compared to sham at 4 h and 24 h*

Metabolites Decreased in AKI	Associated Metabolic Pathway	Fold Change*	Sham vs. AKI *P* Value**
	4 h		
2-Hydroxyglutarate/citralmalate	TCA	0.69	<0.0001
D-Ribitol 5-phosphate	Pentose phosphate pathway	0.53	0.003
S-adenosyl-L-methionine	Amino acid metabolite	0.58	0.006
Lactate	Glycolysis	0.71	0.01
Adenine	Purine derivative	0.83	0.02
Adenosine	Purine derivative	0.69	0.03
Malate	TCA cycle	0.65	0.04
Glutathione disulfide	Glutathione homeostasis	0.44	0.05
Gamma-L-glutamyl-D-alanine	Glutathione homeostasis	0.42	0.05
Leucine/Isoleucine	Amino acid	0.62	0.06
Nicotinamide	Purine metabolite	0.68	0.07
Guanine	Purine nucleobase	0.67	0.07
5-Oxoproline	Glutathione homeostasis	0.70	0.08
5-L-glutamyl-glutamine	Glutathione homeostasis	0.63	0.09
Uracil	Pyrimidine metabolism	0.75	0.09
	24 h		
Adrenaline	Amino acid metabolite	0.50	0.0005
Glutamate	Amino acid	0.56	0.0005
Thioredoxin disulfide	Thioredoxin metabolism/Antioxidant	0.78	0.0006
Carnitine	Organic acid/Amino acid detoxification	0.55	0.002
Lysine	Amino acid	0.69	0.003
Alanine	Amino acid	0.57	0.004
Glutathione (GSH)	Glutathione homeostasis/Antioxidant	0.53	0.005
Valine	Amino acid	0.53	0.005
Aspartate	Amino acid	0.60	0.006
Hypotaurine	Amino acid metabolite	0.41	0.006
Phopshoserine	Amino acid metabolite	0.45	0.02
Cys-Gly	Glutathione synthesis	0.59	0.02
Propanoylcarnitine	Organic acid/Amino acid catabolism	0.54	0.02
Tyrosine	Amino acid	0.57	0.03
Pyridoxamine	Vitamin B6 metabolism	0.74	0.04
Guanine	Purine nucleobase	0.72	0.07
Guanosine	Purine metabolite	0.59	0.08

AKI, acute kidney injury. *Based on median value for peak area. **ANOVA with Sidak multiple comparison test of autoscaled data.

and severity of ARDS (56). Thus, depletion of lung glutathione levels during AKI is a biologically plausible mechanism to explain the increased susceptibility and severity of pulmonary complications in patients with AKI.

In the present study, evidence of the upregulation of alternative energy sources was substantial and included changes in amino acid levels, the TCA cycle, glycolysis, PPP and nucleotide metabolism. AKI is often described as a hypercatabolic state, which is particularly evident in our study since the depletion of amino acids and changes in amino acid metabolites was observed in the lung at all time points. Amino acid depletion may be a result increased metabolism in order to supply nitrogen, which is known to be affected in AKI (57). Altered amino acids and metabolite levels may also suggest upregulation of anaplerosis, which provides carbons from amino acids to the TCA cycle to replenish or maintain ATP levels. Pathway enrichment analysis demonstrating lysine degradation further supports the notion of increased TCA cycle activity and upregulation of alternative sources of ATP generation during AKI. Lysine degradation itself yields glutamate and terminates into acetyl-CoA, of which both are primary contributors to the TCA cycle. Pathway enrichment analysis also demonstrated that the PPP was upregulated at all time points after AKI. Although not nearly as efficient as oxidative phosphorylation, the pentose phosphate pathway does lead to the generation of ATP. Of note, activation of the PPP could also be an effort to increase reducing equivalents in the form of NADPH to increase supply of reduced glutathione. Conversion of oxidized glutathione (GSSG) to the reduced form (GSH) requires NADPH, a cofactor for glutathione reductase which facilitates this reaction. The reduced form of glutathione (GSH) is the form that functions as an antioxidant. Thus, activation of the PPP marks a response to cellular oxidation as is known in other cell types (58). Finally, increased nucleotide metabolism is commonly associated with ATP depletion and efforts to replenish it via alternate energy pathways. As known constituents of ATP, we hypothesize adenosine and adenine were depleted as a result of their use in ATP regeneration. In sum, the effect of AKI on energy metabolism suggest that AKI has an adverse effect on oxidative phosphorylation resulting in the use of other energy pathways to generate ATP.

Limitations

Although our study has several strengths, including the sample size (n = 10) which is within the accepted group size based on recent peer literature of animal-based metabolomics studies (59–62), there are a number of limitations that are important to mention. First, drop-out was observed in the 7-day sham and 7-day AKI groups. However, in this present study, we consider this to be a minor limitation, as we focus the majority of our conclusions and discussion on the changes at 4 and 24 h. Second, the study design was exploratory in nature to identify metabolites that are altered in response to AKI. Third, metabolite levels reported reflect

Table 2. *Metabolites increased in AKI compared to sham at 4 h, 24 h, and 7 days*

Metabolites Increased in AKI	Associated Metabolic Pathway	Fold Change*	Sham vs. AKI *P* Value**
	4 h		
Homocarnosine	Amino acid metabolite	1.53	0.0002
Allantoin	Purine metabolite	2.66	0.002
	24 h		
Creatinine	Arginine and proline metabolism	5.88	<0.0001
D-Ribose	Pentose phosphate pathway	4.24	<0.0001
Homocarnosine	Amino acid metabolite	2.39	<0.0001
L-arabinose	Pentose phosphate pathway	4.24	<0.0001
N-6-methyl-L-lysine	Amino acid metabolite	2.07	<0.0001
N-amidino-L-aspartate	Amino acid metabolite	5.97	<0.0001
Phosphocreatine	Amino acid/Energy metabolite	1.97	<0.0001
Putrescine	Amino acid metabolite	2.61	<0.0001
Allantoin	Purine metabolism	19.95	<0.0001
4-Pyridoxate	Vitamin B6 metabolism	1.63	0.0003
D-Glucose	Glycolysis	2.16	0.004
Ethanolamine phosphate	Glycerophospholipid biosynthesis	1.09	0.006
2-Aminoapidate	Amino acid metabolite	1.27	0.007
5-6-Dihydrothymine	Pyrimidine metabolite	1.28	0.008
2-Oxogluteramate	TCA cycle	1.21	0.05
	7 days		
5-6-Dihydrothymine	Pyrimidine metabolite	1.53	<0.0001
N-6-methyl-L-lysine	Amino acid	2.30	0.0002
Pantothenol	Vitamin B5 metabolism	1.71	0.0009
Ribose	Pentose phosphate pathway	2.81	0.004
N-amidino-L-aspartate	Amino acid metabolite	4.39	0.004
L-arabinose	Pentose phosphate pathway	2.77	0.006
Phosphocreatine	Amino acid/Energy metabolite	1.61	0.006

AKI, acute kidney injury.*Based on median value for peak area.**ANOVA with Sidak multiple comparison test of autoscaled data.

steady state levels that are the cumulative effect of numerous interconnected pathways. Therefore, definitive assessment of substrate sources for key metabolites and metabolic pathways requires additional focused experimentation. Finally, since whole lung was examined, the contribution of individual cell types to changes in energy metabolism is unknown and blood contamination might potentially affect results (although the distinct energy phenotype of the lung versus the kidney and heart argues against this possibility). Thus, these studies are hypothesis generating, serving as a platform for future inquiry. Raw datasets are available for review upon request.

Conclusions

AKI is a complex, systemic disease associated with increased mortality that is likely a consequence of deleterious multiorgan effects. The effect of AKI on the lung is particularly consequential. This is the first study of energy metabolism in the lung after AKI and our findings demonstrate evidence of increased oxidative stress, the use of alternative energy sources, and ATP depletion. We suggest that these metabolic disturbances are plausible mechanisms to explain the increased incidence of pulmonary complications that occur in patients with AKI. The data in this report add novel information to the growing literature demonstrating the adverse effects of AKI on the lung.

Table 3. *Pathway analysis for AKI versus sham*

Time Point/Metabolic Pathway	Hits	Holm-Adjusted *P* Value*
4 h		
Pentose and glucuronate interconversions	3	0.02
24 h		
Lysine degradation	2	0.004
Pentose and glucuronate interconversions	3	0.04
7 days		
Pentose and glucuronate interconversions	3	0.03
Starch and sucrose metabolism	2	0.04

AKI, acute kidney injury. *A pathway was considered significant if the number of significant metabolite hits was 2 or more and the Holm-adjusted *P* value was less than 0.05.

SUPPLEMENTAL DATA

Supplemental Fig. S1: https://doi.org/10.6084/m9.figshare.13299593.

Supplemental Tables S1–S7: https://doi.org/10.6084/m9.figshare.13299593.

ACKNOWLEDGMENTS

The authors thank Matthew J. Winter for assistance with the isolation and preparation of samples for metabolomics analysis.

GRANTS

This work was supported in part by National Heart, Lung, and Blood Institute Grants 1R01HL095363 and 1R01HL130084-01 to S.F.

DISCLOSURES

No conflicts of interest, financial or otherwise, are declared by the authors.

AUTHOR CONTRIBUTIONS

J.A.R. and S.F. conceived and designed research; H.-W.G., C.A., and R.A.B. performed experiments; H.-W.G., B.F., and R.A.B. analyzed data; S.L.A., B.P., P.R.B., J.A.R., and S.F. interpreted results

of experiments; S.L.A., J.A.R., and S.F. prepared figures; S.L.A. drafted manuscript; S.L.A., B.P., P.R.B., J.A.R., and S.F. edited and revised manuscript; S.L.A., J.A.R., and S.F. approved final version of manuscript.

REFERENCES

1. **Uchino S**, **Bellomo R**, **Goldsmith D**, **Bates S**, **Ronco C.** An assessment of the RIFLE criteria for acute renal failure in hospitalized patients. *Crit Care Med* 34: 1913–1917, 2006. doi:10.1097/01.CCM.0000224227.70642.4F.
2. **Star RA.** Treatment of acute renal failure. *Kidney Int* 54: 1817–1831, 1998. doi:10.1046/j.1523-1755.1998.00210.x.
3. **Thakar CV**, **Christianson A**, **Freyberg R**, **Almenoff P**, **Render ML.** Incidence and outcomes of acute kidney injury in intensive care units: a Veterans Administration study. *Crit Care Med* 37: 2552–2558, 2009. doi:10.1097/CCM.0b013e3181a5906f.
4. **Waikar SS**, **Liu KD**, **Chertow GM.** Diagnosis, epidemiology and outcomes of acute kidney injury. *Clin J Am Soc Nephrol* 3: 844–861, 2008. doi:10.2215/CJN.05191107.
5. **Awad AS**, **Okusa MD.** Distant organ injury following acute kidney injury. *Am J Physiol Renal Physiol* 293: F28–F29, 2007. doi:10.1152/ajprenal.00159.2007.
6. **Elapavaluru S**, **Kellum JA.** Why do patients die of acute kidney injury? *Acta Clin Belg Suppl* 62: 326–331, 2007. doi:10.1179/acb.2007.074.
7. **Konstantine KM**, **Mark D**, **Okusa MD.** Distant organ effects of acute kidney injury. *Nephrology Self-Assessment Program* 8, May 2009.
8. **Lee SA**, **Cozzi M**, **Bush EL**, **Rabb H.** Distant organ dysfunction in acute kidney injury: a review. *Am J Kidney Dis* 72: 846–856, 2018. doi:10.1053/j.ajkd.2018.03.028.
9. **Murugan R**, **Kellum JA.** Acute kidney injury: what's the prognosis? *Nat Rev Nephrol* 7: 209–217, 2011. doi:10.1038/nrneph.2011.13.
10. **Teixeira JP**, **Ambruso S**, **Griffin BR**, **Faubel S.** Pulmonary consequences of acute kidney injury. *Semin Nephrol* 39: 3–16, 2019. doi:10.1016/j.semnephrol.2018.10.001.
11. **Liu KD**, **Altmann C**, **Smits G**, **Krawczeski CD**, **Edelstein CL**, **Devarajan P**, **Faubel S.** Serum interleukin-6 and interleukin-8 are early biomarkers of acute kidney injury and predict prolonged mechanical ventilation in children undergoing cardiac surgery: a case-control study. *Crit Care* 13: R104, 2009. doi:10.1186/cc7940.
12. **Metnitz PG**, **Krenn CG**, **Steltzer H**, **Lang T**, **Ploder J**, **Lenz K**, **Le GJ**, **Druml W.** Effect of acute renal failure requiring renal replacement therapy on outcome in critically ill patients. *Crit Care Med* 30: 2051–2058, 2002. doi:10.1097/00003246-200209000-00016.
13. **Vieira JM, Jr.**, **Castro I**, **Curvello-Neto A**, **Demarzo S**, **Caruso P**, **Pastore L, Jr.**, **Imanishe MH**, **Abdulkader RC**, **Deheinzelin D.** Effect of acute kidney injury on weaning from mechanical ventilation in critically ill patients. *Crit Care Med* 35: 184–191, 2007. doi:10.1097/01.CCM.0000249828.81705.65.
14. **Waikar SS**, **Liu KD**, **Chertow GM.** The incidence and prognostic significance of acute kidney injury. *Curr Opin Nephrol Hypertens* 16: 227–236, 2007. doi:10.1097/MNH.0b013e3280dd8c35.
15. **Walcher A**, **Faubel S**, **Keniston A**, **Dennen P.** In critically ill patients requiring CRRT, AKI is associated with increased respiratory failure and death versus ESRD. *Ren Fail* 33: 935–942, 2011. doi:10.3109/0886022X.2011.615964.
16. **Faubel S**, **Shah PB.** Immediate consequences of acute kidney injury: the impact of traditional and nontraditional complications on mortality in acute kidney injury. *Adv Chronic Kidney Dis* 23: 179–185, 2016. doi:10.1053/j.ackd.2016.02.007.
17. **Bleyl U**, **Sander E**, **Schindler T.** The pathology and biology of uremic pneumonitis. *Intensive Care Med* 7: 193–202, 1981. doi:10.1007/BF01724840.
18. **Faubel S.** Pulmonary complications after acute kidney injury. *Adv Chronic Kidney Dis* 15: 284–296, 2008. doi:10.1053/j.ackd.2008.04.008.
19. **Bass HE**, **Greenberg D**, **Singer E**, **Miller MA.** Pulmonary changes in uremia. *Bull N Y Acad Med* 27: 397, 1951.
20. **Heidland A**, **Heine H**, **Heidbreder E**, **Haunschild J**, **Weipert J**, **Gilge U**, **Kluger G**, **Horl WH.** Uremic pneumonitis. evidence for participation of proteolytic enzymes. *Contrib Nephrol* 41: 352–366, 1984.
21. **Hopps HC**, **Wissler RW.** Uremic pneumonitis. *Am J Pathol* 31: 261–273, 1955.
22. **Zettergren L.** Uremic lung; report of four cases reaching autopsy. *Acta Soc Med Ups* 60: 161–171, 1955.
23. **Rogers LK**, **Cismowski MJ.** Oxidative stress in the lung - the essential paradox. *Curr Opin Toxicol* 7: 37–43, 2018. doi:10.1016/j.cotox.2017.09.001.
24. **Kellner M**, **Noonepalle S**, **Lu Q**, **Srivastava A**, **Zemskov E**, **Black SM.** ROS signaling in the pathogenesis of acute lung injury (ALI) and acute respiratory distress syndrome (ARDS). *Adv Exp Med Biol* 967: 105–137, 2017. doi:10.1007/978-3-319-63245-2_8.
25. **Dong Z**, **Yuan Y.** Accelerated inflammation and oxidative stress induced by LPS in acute lung injury: inhibition by ST1926. *Int J Mol Med* 41: 3405–3421, 2018. doi:10.3892/ijmm.2018.3574.
26. **Fu C**, **Dai X**, **Yang Y**, **Lin M**, **Cai Y**, **Cai S.** Dexmedetomidine attenuates lipopolysaccharide-induced acute lung injury by inhibiting oxidative stress, mitochondrial dysfunction and apoptosis in rats. *Mol Med Rep* 15: 131–138, 2017. doi:10.3892/mmr.2016.6012.
27. **Nagato AC**, **Bezerra FS**, **Lanzetti M**, **Lopes AA**, **Silva MA**, **Porto LC**, **Valenca SS.** Time course of inflammation, oxidative stress and tissue damage induced by hyperoxia in mouse lungs. *Int J Exp Path* 93: 269–278, 2012. doi:10.1111/j.1365-2613.2012.00823.x.
28. **Zhao W**, **Zhou S**, **Yao W**, **Gan X**, **Su G**, **Yuan D**, **Hei Z.** Propofol prevents lung injury after intestinal ischemia-reperfusion by inhibiting the interaction between mast cell activation and oxidative stress. *Life Sci* 108: 80–87, 2014. doi:10.1016/j.lfs.2014.05.009.
29. **Bassett DJ**, **Fisher AB.** Metabolic response to carbon monoxide by isolated rat lungs. *Am J Physiol* 230: 658–663, 1976. doi:10.1152/ajplegacy.1976.230.3.658.
30. **Serkova NJ**, **Van Rheen Z**, **Tobias M**, **Pitzer JE**, **Wilkinson JE**, **Stringer KA.** Utility of magnetic resonance imaging and nuclear magnetic resonance-based metabolomics for quantification of inflammatory lung injury. *Am J Physiol Lung Cell Mol Physiol* 295: L152–L161, 2008. doi:10.1152/ajplung.00515.2007.
31. **Tojo K**, **Tamada N**, **Nagamine Y**, **Yazawa T**, **Ota S**, **Goto T.** Enhancement of glycolysis by inhibition of oxygen-sensing prolyl hydroxylases protects alveolar epithelial cells from acute lung injury. *FASEB J* 32: 2258–2268, 2018. doi:10.1096/fj.201700888R.
32. **Yang H**, **Sun R**, **Ma N**, **Liu Q**, **Sun X**, **Zi P**, **Wang J**, **Chao K**, **Yu L.** Inhibition of nuclear factor-kappaB signal by pyrrolidine dithiocarbamate alleviates lipopolysaccharide-induced acute lung injury. *Oncotarget* 8: 47296–47304, 2017. doi:10.18632/oncotarget.17624.
33. **Klein CL**, **Hoke TS**, **Fang WF**, **Altmann CJ**, **Douglas IS**, **Faubel S.** Interleukin-6 mediates lung injury following ischemic acute kidney injury or bilateral nephrectomy. *Kidney Int* 74: 901–909, 2008. doi:10.1038/ki.2008.314.
34. **Fox BM**, **Gil HW**, **Kirkbride-Romeo L**, **Bagchi RA**, **Wennersten SA**, **Haefner KR**, **Skrypnyk NI**, **Brown CN**, **Soranno DE**, **Gist KM**, **Griffin BR**, **Jovanovich A**, **Reisz JA**, **Wither MJ**, **D'Alessandro A**, **Edelstein CL**, **Clendenen N**, **McKinsey TA**, **Altmann C**, **Faubel S.** Metabolomics assessment reveals oxidative stress and altered energy production in the heart after ischemic acute kidney injury in mice. *Kidney Int* 95: 590–610, 2019. doi:10.1016/j.kint.2018.10.020.
35. **Nemkov T**, **Reisz JA**, **Gehrke S**, **Hansen KC**, **D'Alessandro A.** High-throughput metabolomics: isocratic and gradient mass spectrometry-based methods. *Methods Mol Biol* 1978: 13–26, 2019. doi:10.1007/978-1-4939-9236-2_2.
36. **Nemkov T**, **Hansen KC**, **D'Alessandro A.** A three-minute method for high-throughput quantitative metabolomics and quantitative tracing experiments of central carbon and nitrogen pathways. *Rapid Commun Mass Spectrom* 31: 66–673, 2017. doi:10.1002/rcm.7834.
37. **Hoke TS**, **Douglas IS**, **Klein CL**, **He Z**, **Fang W**, **Thurman JM**, **Tao Y**, **Dursun B**, **Voelkel NF**, **Edelstein CL**, **Faubel S.** Acute renal failure after bilateral nephrectomy is associated with cytokine-mediated pulmonary injury. *J Am Soc Nephrol* 18: 155–164, 2007. doi:10.1681/ASN.2006050494.
38. **Pang Z**, **Chong J**, **Li S**, **Xia J.** MetaboAnalystR 3.0: toward an optimized workflow for global metabolomics. *Metabolites* 10: 186, 2020. doi:10.3390/metabo10050186.
39. **Skrypnyk NI**, **Gist KM**, **Okamura K**, **Montford JR**, **You Z**, **Yang H**, **Moldovan R**, **Bodoni E**, **Blaine JT**, **Edelstein CL**, **Soranno DE**, **Kirkbride-Romeo LA**, **Griffin BR**, **Altmann C**, **Faubel S.** IL-6-mediated hepatocyte production is the primary source of plasma and

urine neutrophil gelatinase-associated lipocalin during acute kidney injury. *Kidney Int* 97: 966–979, 2019. doi:10.1016/j.kint.2019.11.013.

40. **Faubel S**, **Ljubanovic D**, **Poole B**, **Dursun B**, **He Z**, **Cushing S**, **Somerset H**, **Gill RG**, **Edelstein CL.** Peripheral CD4 T-cell depletion is not sufficient to prevent ischemic acute renal failure. *Transplantation* 80: 643–649, 2005. doi:10.1097/01.tp.0000173396.07368.55.
41. **Altmann C**, **Ahuja N**, **Kiekhaefer CM**, **Andres -Hernando A**, **Okamura K**, **Bhargava R**, **Duplantis J**, **Kirkbride-Romeo LA**, **Huckles J**, **Fox BM**, **Kahn K**, **Soranno D**, **Gil HW**, **Teitelbaum I**, **Faubel S.** Early peritoneal dialysis reduces lung inflammation in mice with ischemic acute kidney injury. *Kidney Int* 92: 365–376, 2017. doi:10.1016/j.kint.2017.01.020.
42. **Andres-Hernando A**, **Altmann C**, **Bhargava R**, **Okamura K**, **Bacalja J**, **Hunter B**, **Ahuja N**, **Soranno D**, **Faubel S.** Prolonged acute kidney injury exacerbates lung inflammation at 7 days post-acute kidney injury. *Physiol Rep* 2: e12084, 2014. doi:10.14814/phy2.12084.
43. **Faubel S**, **Edelstein CL.** Mechanisms and mediators of lung injury after acute kidney injury. *Nat Rev Nephrol* 12: 48–60, 2016. doi:10.1038/nrneph.2015.158.
44. **Grams ME**, **Rabb H.** The distant organ effects of acute kidney injury. *Kidney Int* 81: 942–948, 2012. doi:10.1038/ki.2011.241.
45. **Awad AS**, **Rouse M**, **Huang L**, **Vergis AL**, **Reutershan J**, **Cathro HP**, **Linden J**, **Okusa MD.** Compartmentalization of neutrophils in the kidney and lung following acute ischemic kidney injury. *Kidney Int* 75: 689–698, 2009. doi:10.1038/ki.2008.648.
46. **Kramer AA**, **Postler G**, **Salhab KF**, **Mendez C**, **Carey LC**, **Rabb H.** Renal ischemia/reperfusion leads to macrophage-mediated increase in pulmonary vascular permeability. *Kidney Int* 55: 2362–2367, 1999. doi:10.1046/j.1523-1755.1999.00460.x.
47. **Lie ML**, **White LE**, **Santora RJ**, **Park JM**, **Rabb H**, **Hassoun HT.** Lung T lymphocyte trafficking and activation during ischemic acute kidney injury. *J Immunol* 189: 2843–2851, 2012. doi:10.4049/jimmunol.1103254.
48. **Nakazawa D**, **Kumar SV**, **Marschner J**, **Desai J**, **Holderied A**, **Rath L**, **Kraft F**, **Lei Y**, **Fukasawa Y**, **Moeckel GW**, **Angelotti ML**, **Liapis H**, **Anders HJ.** Histones and neutrophil extracellular traps enhance tubular necrosis and remote organ injury in ischemic AKI. *J Am Soc Nephrol* 28: 1753–1768, 2017. doi:10.1681/ASN.2016080925.
49. **Hassoun HT**, **Lie ML**, **Grigoryev DN**, **Liu M**, **Tuder RM**, **Rabb H.** Kidney ischemia-reperfusion injury induces caspase-dependent pulmonary apoptosis. *Am J Physiol Renal Physiol* 297: F125–F137, 2009. doi:10.1152/ajprenal.90666.2008.
50. **Pollyea DA**, **Stevens BM**, **Jones CL**, **Winters A**, **Pei S**, **Minhajuddin M**, **D'Alessandro A**, **Culp-Hill R**, **Riemondy KA**, **Gillen AE**, **Hesselberth JR**, **Abbott D**, **Schatz D**, **Gutman JA**, **Purev E**, **Smith C**, **Jordan CT.** Venetoclax with azacitidine disrupts energy metabolism and targets leukemia stem cells in patients with acute myeloid leukemia. *Nat Med* 24: 1859–1866, 2018. doi:10.1038/s41591-018-0233-1.
51. **Andres-Hernando A**, **Dursun B**, **Altmann C**, **Ahuja N**, **He Z**, **Bhargava R**, **Edelstein CE**, **Jani A**, **Hoke TS**, **Klein C**, **Faubel S.** Cytokine production increases and cytokine clearance decreases in mice with bilateral nephrectomy. *Nephrol Dial Transplant* 27: 4339–4347, 2012. doi:10.1093/ndt/gfs256.
52. **Dennen P**, **Altmann C**, **Kaufman J**, **Klein CL**, **Andres-Hernando A**, **Ahuja NH**, **Edelstein CL**, **Cadnapaphornchai MA**, **Keniston A**, **Faubel S.** Urine interleukin-6 is an early biomarker of acute kidney injury in children undergoing cardiac surgery. *Crit Care* 14: R181, 2010. doi:10.1186/cc9289.
53. **Klein CL**, **Hoke TS**, **Fang WF**, **Altmann CJ**, **Douglas IS**, **Faubel S.** Interleukin-6 mediates lung injury following ischemic acute kidney injury or bilateral nephrectomy. *Kidney Int* 74: 901–909, 2008. doi:10.1038/ki.2008.314.
54. **Ahuja N**, **Andres-Hernando A**, **Altmann C**, **Bhargava R**, **Bacalja J**, **Webb RG**, **He Z**, **Edelstein CL**, **Faubel S.** Circulating IL-6 mediates lung injury via CXCL1 production after acute kidney injury in mice. *Am J Physiol Renal Physiol* 303: F864–F872, 2012. doi:10.1152/ajprenal.00025.2012.
55. **Glund S**, **Deshmukh A**, **Long YC**, **Moller T**, **Koistinen HA**, **Caidahl K**, **Zierath JR**, **Krook A.** Interleukin-6 directly increases glucose metabolism in resting human skeletal muscle. *Diabetes* 56: 1630–1637, 2007. doi:10.2337/db06-1733.
56. **Moss M**, **Guidot DM**, **Wong-Lambertina M**, **Ten HT**, **Perez RL**, **Brown LA.** The effects of chronic alcohol abuse on pulmonary glutathione homeostasis. *Am J Respir Crit Care Med* 161: 414–419, 2000. doi:10.1164/ajrccm.161.2.9905002.
57. **Fiaccadori E**, **Regolisti G**, **Cabassi A.** Specific nutritional problems in acute kidney injury, treated with non-dialysis and dialytic modalities. *NDT Plus* 3: 1–7, 2010. doi:10.1093/ndtplus/sfp017.
58. **Reisz JA**, **Wither MJ**, **Dzieciatkowska M**, **Nemkov T**, **Issaian A**, **Yoshida T**, **Dunham AJ**, **Hill RC**, **Hansen KC**, **D'Alessandro A.** Oxidative modifications of glyceraldehyde 3-phosphate dehydrogenase regulate metabolic reprogramming of stored red blood cells. *Blood* 128: e32–e42, 2016. doi:10.1182/blood-2016-05-714816.
59. **Chandler JD**, **Hu X**, **Ko EJ**, **Park S**, **Lee YT**, **Orr M**, **Fernandes J**, **Uppal K**, **Kang SM**, **Jones DP**, **Go YM.** Metabolic pathways of lung inflammation revealed by high-resolution metabolomics (HRM) of H1N1 influenza virus infection in mice. *Am J Physiol Regul Integr Comp Physiol* 311: R906–R916, 2016. doi:10.1152/ajpregu.00298.2016.
60. **Levy BD**, **Abdulnour RE**, **Tavares A**, **Bruggemann TR**, **Norris PC**, **Bai Y**, **Ai X**, **Serhan CN.** Cysteinyl maresins regulate the prophlogistic lung actions of cysteinyl leukotrienes. *J Allergy Clin Immunol* 145: 335–344, 2020. doi:10.1016/j.jaci.2019.09.028.
61. **Qian W**, **Kang A**, **Peng L**, **Xie T**, **Ji J**, **Zhou W**, **Shan J**, **Di L.** Gas chromatography-mass spectrometry based plasma metabolomics of H1N1-induced inflammation in mice and intervention with Flos Lonicerae Japonica-Fructus Forsythiae herb pair. *J Chromatogr B Analyt Technol Biomed Life Sci* 1092: 122–130, 2018. doi:10.1016/j.jchromb.2018.05.047.
62. **Showalter MR**, **Nonnecke EB**, **Linderholm AL**, **Cajka T**, **Sa MR**, **Lonnerdal B**, **Kenyon NJ**, **Fiehn O.** Obesogenic diets alter metabolism in mice. *PLoS One* 13: e0190632, 2018. doi:10.1371/journal.pone.0190632.